Journal of Photonics for Energy

PhotonicsforEnergy.SPIEDigitalLibrary.org

Evaluation of ambipolar carrier mobility in alkyl-substituted phthalocyanine thin film

Yuki Nishikawa
Yuya Nakata
Shigehiro Ikehara
Akihiko Fujii
Masanori Ozaki

SPIE.

Yuki Nishikawa, Yuya Nakata, Shigehiro Ikehara, Akihiko Fujii, Masanori Ozaki, "Evaluation of ambipolar carrier mobility in alkyl-substituted phthalocyanine thin film," *J. Photon. Energy* **8**(3), 032214 (2018), doi: 10.1117/1.JPE.8.032214.

Evaluation of ambipolar carrier mobility in alkyl-substituted phthalocyanine thin film

Yuki Nishikawa, Yuya Nakata, Shigehiro Ikehara, Akihiko Fujii,* and Masanori Ozaki
Osaka University, Division of Electrical, Electronic and Information Engineering, Graduate School of Engineering, Osaka, Japan

Abstract. Ambipolar carrier mobility in a thin film of hexyl-substituted phthalocyanine ($C6PcH_2$), which is a promising donor material for solution-processed organic thin-film solar cells, has been studied by measuring photogenerated charge carriers extracted under a linearly increasing voltage. As the extraction transient current of the $C6PcH_2$ thin film could not be observed in a conventional device structure composed of a single organic layer, an evaporated layer of C_{60} or pentacene was introduced as a charge-separation layer to determine the hole or electron mobility, respectively. An extraction transient current clearly appeared owing to the efficient photo-induced charge generation at the interface between the $C6PcH_2$ and charge-separation layers. The hole and electron mobilities were evaluated by a proposed analytical model, which took into account the carrier generation at the interface and the carrier diffusion during the delay time. © *2018 Society of Photo-Optical Instrumentation Engineers (SPIE)* [DOI: 10.1117/1.JPE.8.032214]

Keywords: organic semiconductor; phthalocyanine; ambipolar carrier transport; photo-CELIV; carrier mobility.

Paper 18021SS received Feb. 20, 2018; accepted for publication Apr. 25, 2018; published online May 15, 2018.

1 Introduction

Solution-processable organic semiconductors have been attracting considerable attention to realize low-cost device applications with desirable characteristics, such as a light weight and flexibility. Recently, small molecular organic semiconductors as well as π-conjugated polymeric materials have been widely studied for use in organic electronics.[1,2] Small molecular organic semiconductors were originally regarded as unsuitable for application to solution-processed devices owing to their poor solubility in typical solvents or their strong molecular cohesiveness in the film state. However, the introduction of substituents into molecules not only enabled small molecules to be dissolved in solvents but also allowed the uniform thin films to be easily fabricated by solution processes including printing methods.

1,4,8,11,15,18,22,25-octahexylphthalocyanine ($C6PcH_2$) is a small molecular organic semiconductor that possesses eight substituents of the alkyl chain at the nonperipheral positions of phthalocyanine. $C6PcH_2$ dissolves in typical organic solvents, and a uniform thin film of $C6PcH_2$ can be easily fabricated by spin-coating or bar-coating.[3,4] $C6PcH_2$ exhibits a liquid crystalline phase and tends to form a columnar structure in both the liquid crystalline and crystal phases.[5–8] As the π-orbitals of phthalocyanine cores tend to overlap in the direction of the column axis in the columnar structure, efficient and uniaxial carrier transport along the column axis is expected. Indeed, the ambipolar high carrier mobility along the column axis of $C6PcH_2$ has been demonstrated, and the hole and electron mobilities of $C6PcH_2$ were estimated to be 1.4 and 0.5 cm^2/Vs, respectively, by time-of-flight (TOF) measurement.[9] $C6PcH_2$ acts as an effective donor material in an organic bulk heterojunction thin-film solar cell, resulting in excellent device

*Address all correspondence to: Akihiko Fujii, E-mail: afujii@eei.eng.osaka-u.ac.jp

1947-7988/2018/$25.00 © 2018 SPIE

performance including a high current density and a high-power conversion efficiency of 4.2%.[10] However, details of the current generation by photoexcitation, particularly the carrier transport in the solar cell, have not been clarified.

The carrier mobility of organic semiconductors has been investigated by various methods, such as TOF, space-charge-limited current (SCLC), and field-effect transistor (FET) methods.[11,12] These methods have some problems in evaluating the carrier mobility in organic thin-film solar cells.[11,12] A film that is at least an order of magnitude thicker than a typical bulk heterojunction active layer in the solar cell is necessary in the TOF method. In the SCLC measurement, an electric field of MV/cm order, which is much higher than the operational condition of solar cells, is applied to the thin film. In the FET measurement, the direction of the carrier motion is parallel to the substrate, whereas it is perpendicular to the substrate in solar cells. Thus, these techniques are not suitable for the precise evaluation of carrier mobility in organic thin-film solar cells.

Photo-induced carrier extraction by a linearly increasing voltage (photo-CELIV) is another mobility measurement technique, which was proposed by Juška et al.[13] Photo-CELIV can be used for 100-nm-order thin-film samples. Moreover, the applied electric field and sample geometry are similar to those of solar cells. Therefore, the photo-CELIV method has been widely used to study the carrier transport in organic solar cells.[14–16]

However, there are some limitations of the conventional photo-CELIV method. As the photocurrent signal has to be sufficiently strong to distinguish it from the dark current, it is difficult to evaluate the carrier mobility of materials with low quantum efficiency of carrier generation by photo-excitation.[17] As described below, conventional photo-CELIV is not applicable to a $C6PcH_2$ single-layer thin film because $C6PcH_2$ has a low quantum efficiency of photogenerated carriers. Moreover, using conventional photo-CELIV, only the majority carriers can be discussed, and their polarity cannot be determined.[13]

In this study, the ambipolar carrier mobility in a $C6PcH_2$ thin film was investigated utilizing the photo-CELIV method. For efficient carrier generation, a charge separation layer, the material of which was selected in accordance with the measurement of hole or electron mobility, was inserted between the $C6PcH_2$ layer and an electrode. The hole and electron mobilities were evaluated by a proposed analytical model, which took into account the carrier generation at the interface and carrier diffusion during the delay time.

2 Experimental Details

The molecular structures of $C6PcH_2$, C_{60}, and pentacene are shown in Fig. 1. $C6PcH_2$ was synthesized and purified as reported previously.[18] C_{60} (Frontier Carbon Corporation) and pentacene (Tokyo Chemical Industry Co., Ltd.) were used as purchased. The configurations of the device used for the photo-CELIV measurement are schematically shown in Fig. 2.

An indium-tin-oxide (ITO) coated glass substrate was cleaned with an alkaline solution and water by ultrasonication, then treated with UV-ozone. To prepare devices A and C in Fig. 2, an aqueous solution of poly(3,4-ethylenedioxythiophene):poly(styrene sulfonate) (PEDOT:PSS) (Baytron P VP AI 4083) was diluted with the same volume of 2-propanol, spin-coated at a speed of 3000 rpm, then dried at 100°C for 10 min in an oven under atmospheric conditions.

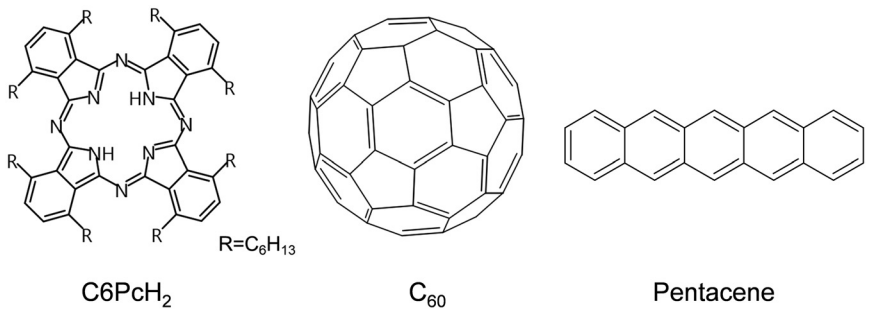

Fig. 1 Molecular structures of $C6PcH_2$, C_{60}, and pentacene.

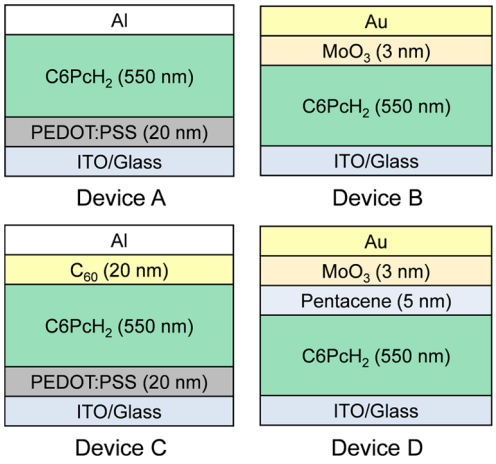

Fig. 2 Schematic device structures for the photo-CELIV measurement.

$C6PcH_2$ was dissolved in chloroform at a concentration of 45 g/L, and the solution was spin-coated onto the substrates at a speed of 500 rpm. The film thickness was estimated to be ~550 nm from the optical absorbance measured using a spectrophotometer (Shimadzu UV-3150). A 20-nm-thick C_{60} film or 5-nm-thick pentacene film, as a charge separation layer, was thermally evaporated at a rate of 0.1 Å/s under a vacuum of about 10^{-4} Pa in devices C and D, respectively. The thickness of C_{60} and pentacene layers was optimized by taking the suppression of the series resistance as well as the efficient charge separation into consideration. As the series resistance of them can be neglected compared with the $C6PcH_2$ layer because of 5 or 20 nm in thickness, the electric field should be mainly applied to the $C6PcH_2$ layer in the electrical measurement using an external source. In the devices B and D, a 3-nm-thick MoO_3 film was thermally evaporated at a rate of 0.1 Å/s under a vacuum of about 10^{-4} Pa. An 80-nm-thick aluminum or gold layer, used as a counter electrode to the ITO electrode, was deposited onto the active layer by thermal evaporation under pressure of ~10^{-4} Pa.

The measurement using the photo-CELIV method was carried out under a vacuum at room temperature. The synchronized beam of a Q-switched neodymium-yttrium-aluminum-garnet pulsed laser (CryLaS FTSS355-50) was irradiated from the ITO-layer side of the devices. The wavelength, pulse width, and pulse repetition rate of the laser were 355 nm, 1 ns, and 20 Hz, respectively. A reverse bias in the form of a triangular pulse was applied between the electrodes using a function generator (NF Corporation WF1973). The delay time between the laser radiation and voltage application was set to 0.65 μs. The generated transient current was recorded using a digital oscilloscope (Teledyne LeCroy HDO4054).

For the photoluminescence (PL) measurement, devices with bilayer structures of $C6PcH_2/C_{60}$ and $C6PcH_2$/pentacene were prepared on a quartz substrate. The thicknesses of $C6PcH_2$, C_{60}, and pentacene were 30, 20, and 20 nm, respectively. A near-infrared spectrofluorometer (JASCO FP-8700) was utilized to measure the PL spectrum, and the wavelength of the excitation light was set to 633 nm, corresponding to the optical transition at the Q band of $C6PcH_2$.

3 Results and Discussion

3.1 *Experimental Results*

Figure 3 shows the absorption spectra of $C6PcH_2$, C_{60} and pentacene thin films. The absorption peak at 355 nm can be seen in the spectrum of the $C6PcH_2$ thin film, and the incident laser pulse must be efficiently absorbed in the $C6PcH_2$ layer for all types of the devices in Fig. 2. By the excitation light irradiation from the ITO-coated substrate side, the exciton should be mainly generated in the $C6PcH_2$ layer.

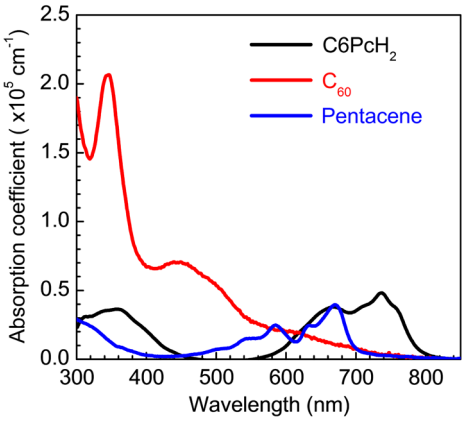

Fig. 3 Absorption spectra of $C6PcH_2$, C_{60}, and pentacene thin films.

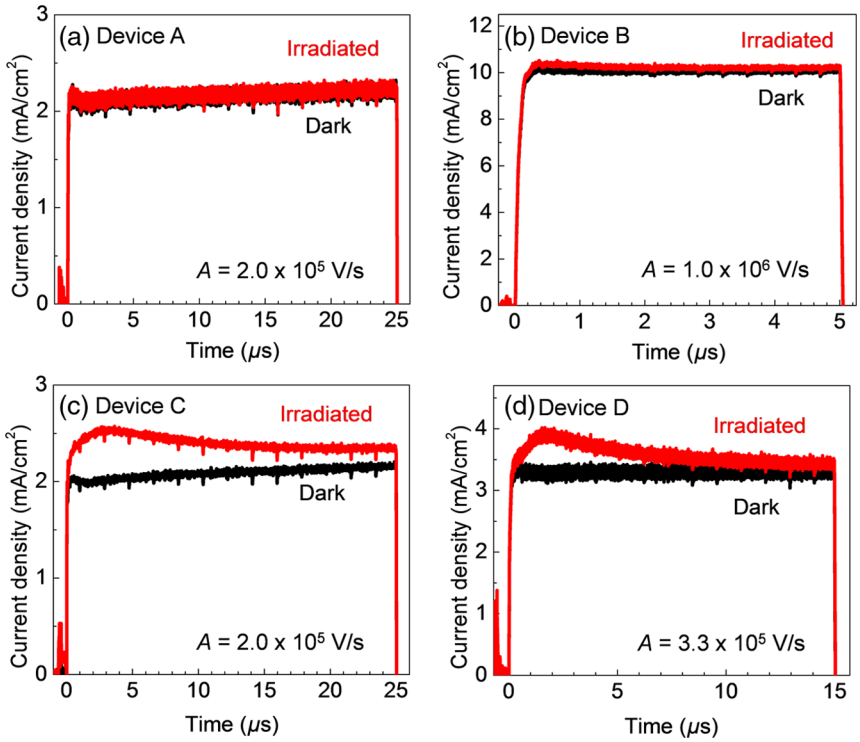

Fig. 4 Typical transient current waveforms of devices of A–D. The black and red lines indicate the dark and irradiated conditions, respectively.

The transient current waveforms obtained in the photo-CELIV measurement of devices A–D are shown in Figs. 4(a)–4(d), respectively. The black and red lines in these figures indicate the dark and irradiated conditions, respectively. For the single-layer devices, such as devices A and B, the current signals under the dark and irradiated conditions appeared to be consistent as shown in Figs. 4(a) and 4(b). Although a laser pulse was irradiated to the $C6PcH_2$ thin films and a linearly increasing voltage was applied, a component originating from photogenerated carriers was not observed from these devices. The pulsed laser irradiation of the films should excite the $C6PcH_2$ molecules to generate excitons; however, the failure to extract photogenerated carriers might have been caused by the low quantum efficiency of carrier generation owing to the large exciton binding energy required to induce exciton dissociation. Consequently, the single-layer film of $C6PcH_2$ was unsuitable for the photo-CELIV measurement.

In contrast, devices C and D, which included charge-separation layers, demonstrated clear current signals originating from carrier extraction under the irradiated condition, in strong

contrast to those under the dark condition, as shown in Figs. 4(c) and 4(d). The photogenerated excitons are migrated in $C6PcH_2$ layer within the exciton diffusion length of $C6PcH_2$, 30 nm.[19] Namely, the excitons generated near the interface of charge separation layer could reach the interface and be dissociated. By introducing the charge-separation layer of C_{60} or pentacene in this study, it is assumed that photogenerated excitons were efficiently dissociated to generate carriers, resulting in the carrier extraction from the devices.

In a bulk heterojunction thin film with a ternary system of $C6PcH_2$, a fullerene derivative, 1-(3-methoxycarbonyl)-propyl-1-1-phenyl-(6,6)C61 (PCBM), and poly(3-hexylthiophene) (P3HT), $C6PcH_2$ behaves as a donor at the interface with PCBM and as an acceptor at the interface with P3HT, as reported previously.[20] Taking note of the highest occupied molecular orbital (HOMO) level and lowest unoccupied molecular orbital (LUMO) level of $C6PcH_2$ and C_{60},[20,21] as shown in Fig. 5(a), it is considered that $C6PcH_2$ acts as a donor material at the interface with C_{60} and that holes are generated and transported in the $C6PcH_2$ layer. The energy diagram of pentacene was determined by the photoelectron spectroscopy and absorption edge of a 50-nm-thick homogeneous pentacene film as shown in Fig. 5(b). At the interface with pentacene, $C6PcH_2$ works as an acceptor material and electrons must be generated and transport in the $C6PcH_2$ layer. That is, hole and electron generation based on photo-induced charge transfer should occur at the $C6PcH_2/C_{60}$ and $C6PcH_2$/pentacene interfaces, respectively.

In a previous study on a thin film with a bulk heterojunction of P3HT and C_{60}, PL quenching was reported as evidence of photo-induced charge transfer.[22] To confirm the photo-induced charge transfer between $C6PcH_2$ and C_{60} and between $C6PcH_2$ and pentacene, PL spectra of $C6PcH_2/C_{60}$ and $C6PcH_2$/pentacene bilayer films were measured. Compared with the PL spectra of the $C6PcH_2$ single-layer films, although the spectral shapes were maintained, the PL intensities were markedly suppressed as shown in Fig. 6. The relative quenching ratios R_{PL} at the peak wavelength of 770 nm, defined as $R_{PL} = 1 -$ (PL intensity with charge separation layer)/(PL intensity without charge separation layer), were 93% for the $C6PcH_2/C_{60}$ bilayer film

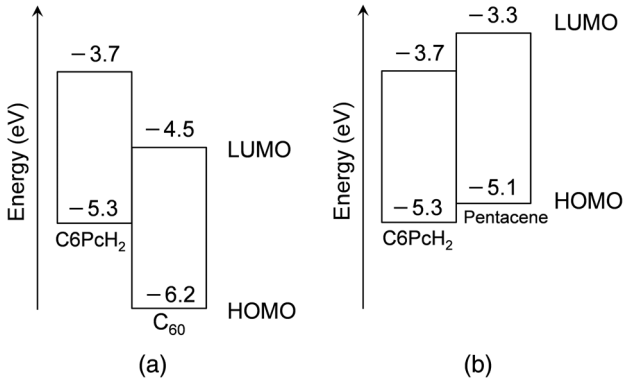

Fig. 5 Energy diagrams of (a) $C6PcH_2/C_{60}$ and (b) $C6PcH_2$/pentacene.

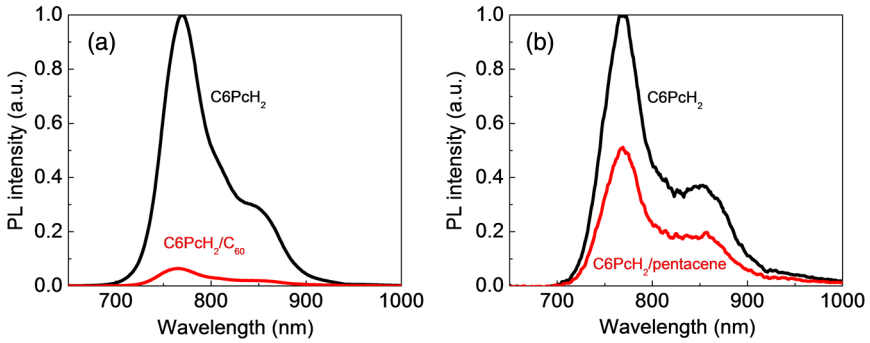

Fig. 6 PL spectra of the bilayer films of (a) $C6PcH_2/C_{60}$ and (b) $C6PcH_2$/pentacene, which are compared with those of the $C6PcH_2$ single-layer films.

and 50% for the C6PcH$_2$/pentacene film. Namely, the R_{PL} in C6PcH$_2$/pentacene bilayer structure was relatively low compared with C6PcH$_2$/C$_{60}$ one. As shown in Fig. 5, the energy offset of LUMO between C6PcH$_2$ and C$_{60}$, which was estimated to be 0.8 eV, was larger than that of HOMO between C6PcH$_2$ and pentacene, which was 0.2 eV. As reported in a previous research,[23] the low-energy offset tends to cause the suppressed yield of the exciton dissociation. Therefore, it is considered that the photo-induced charge transfer at the C6PcH$_2$/pentacene interface was not as efficient as that at the C6PcH$_2$/C$_{60}$ interface.

Thus, the PL quenching as well as the transient current signals in photo-CELIV indicate that the carrier generation owing to photo-excitation was effectively caused by installing the charge-separation layers. Moreover, although the transient current waveforms appeared to be similar in Figs. 4(c) and 4(d), the current signals observed for the C6PcH$_2$/C$_{60}$ and C6PcH$_2$/pentacene bilayer films indicate the transport of holes and electrons, respectively.

3.2 *Theoretical Analysis*

In a conventional photo-CELIV measurement, the photogenerated carriers are assumed to exist with a distribution depending on the light absorption in the bulk film, and the carrier mobility is estimated using previously reported equations. [13,24] In the bilayer structure adopted in this study, the carriers should be generated locally at the interface between the C6PcH$_2$ and the charge-separation layers and diffused from the interface during the delay time until the voltage application. Then, the carriers start to be extracted by the linearly increasing voltage; therefore, the initial carrier distribution in this case is different from that in conventional studies. To evaluate the carrier mobility of C6PcH$_2$ in the bilayer structures, theoretical derivation should be proposed.

In this study, the carrier distribution is defined as $n(x,t)$, which is a function of the position x in the C6PcH$_2$ layer from the interface with the charge-separation layer and time t. Here, it is assumed that the sheet carriers are generated just after the laser pulse irradiation. The pulsed laser is irradiated to the device at $t=-t_{del}$, and the linearly increasing voltage starts to be applied at $t=0$. Therefore, the distribution of generated carriers shortly after the laser pulse irradiation is expressed as

$$n(x,-t_{del})=N_0\delta(x), \tag{1}$$

where N_0 is the total number of generated carriers and $\delta(x)$ is the Dirac delta function.

After the generation of sheet carriers, the carriers diffuse in accordance with the diffusion equation

$$\frac{\partial n}{\partial t}=D\frac{\partial^2 n}{\partial x^2}, \tag{2}$$

where D is the diffusion constant, which follows Einstein's law:

$$D=\frac{\mu kT}{e}, \tag{3}$$

where μ is the carrier mobility, k is the Boltzmann constant, T is the temperature, and e is the elementary charge. By solving Eq. (2) with Eqs. (1) and (3), the initial carrier distribution can be expressed as

$$n(x,0)=\frac{N_0}{2\sqrt{Dt_{del}\pi}}e^{-\frac{x^2}{4Dt_{del}}}. \tag{4}$$

Although the linearly increasing voltage is applied, the carriers are assumed to drift at a velocity of

$$v(t)=\mu E(x,t)=\mu At/d, \tag{5}$$

where $E(x,t)$ is the electric field, A is the slope of the applied triangular voltage pulse, and d is the thickness of the C6PcH$_2$ layer. Then, the carrier distribution can be expressed as

$$n(x,t) = \begin{cases} \frac{N_0}{2\sqrt{Dt_{\mathrm{del}}\pi}} e^{-\frac{(x-l(t))^2}{4Dt_{\mathrm{del}}}} & [l(t) \le x \le d] \\ 0 & (\text{otherwise}) \end{cases}, \tag{6}$$

where $l(t) = \int_0^t v(t')\mathrm{d}t'$ is the extraction depth.[25]

The time-dependent current $j(t)$ can be expressed as[13,25]

$$j(t) = \frac{\varepsilon\varepsilon_0 A}{d} + \frac{\mu e}{d}\int_{l(t)}^{d} n(x,t)E(x,t)\mathrm{d}x, \tag{7}$$

where ε and ε_0 are the relative and vacuum permittivities, respectively. Then, the peak time $t_{\max}$ in the extraction transient current waveform can be obtained by differentiating Eq. (7) with respect to t, by setting it to zero as $\partial j/\partial t = 0$ and solving it for t. However, as this equation cannot be solved analytically, the fitting of the calculated $t_{\max}$ as a function of A to the experimental results was carried out as shown in Fig. 7. The red rhomboid symbols and black lines in Fig. 7 indicate the experimental data and calculated values, respectively. By optimizing the parameter μ, the experimental results were successfully reproduced. Using the proposed analytical formulation, the hole and electron mobilities in the C6PcH$_2$ thin film were evaluated to be 1.5×10^{-3} and 2.1×10^{-3} cm^2/Vs, respectively.

In conventional studies employing the photo-CELIV method, the following equation is generally utilized to determine the carrier mobility.[16]

$$\mu = K\frac{d^2}{At_{\max}^2}, \tag{8}$$

where $K = 2/3$ for the volume initial carrier distribution and $K = 2$ for the surface initial carrier distribution. The hole and electron mobilities obtained by Eq. (8) with $K = 2/3$ were 9.7×10^{-4} and 1.4×10^{-3} cm^2/Vs, whereas those obtained by Eq. (8) with $K = 2$ were 2.9×10^{-3} and 4.3×10^{-3}cm^2/Vs, respectively. In our proposed method, the initial carrier distribution was taken into account, as expressed by Eq. (4); this implies that the estimated values are based on the intermediate condition between the volume and surface carrier distributions in the conventional equation of Eq. (8).

Both the hole and electron mobilities obtained in this study are approximately 10^3 times lower than those evaluated by TOF measurement.[9] This difference in the mobility is strongly related to the molecular alignment in the devices utilized in the photo-CELIV and TOF measurements. A sandwich-cell-type device is mainly utilized in TOF measurement for columnar LC materials, and the column axis of C6PcH$_2$ is reported to be tilted from the normal direction to the substrate.[26] In contrast, the column axis direction in spin-coated C6PcH$_2$ films is reported to be exactly parallel to the substrate.[6] Thus, the carrier mobility in the intercolumn direction can be

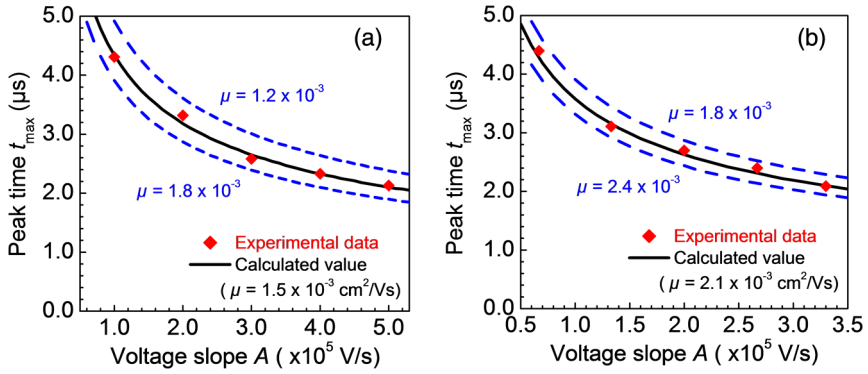

Fig. 7 Peak time $t_{\max}$ of the experimental results as a function of voltage slope A and fitting line by numerical calculation for devices of (a) C and (b) D. Blue broken lines are by numerical calculation with slightly shifted values of μ.

evaluated by the photo-CELIV technique using a bilayer structure, which should provide important information on the ambipolar carrier transport in thin films.

4 Conclusions

The ambipolar carrier mobility in a C6PcH_2 thin film was studied using the photo-CELIV method. The introduction of a charge-separation layer of C_{60} or pentacene enabled to obtain the extraction transient current waveforms of the C6PcH_2 thin film. The ambipolar carrier mobility was successfully evaluated by a numerical calculation using the proposed model taking into account the carrier generation at the interface with the charge-separation layer and the carrier diffusion during the delay time between the laser irradiation and voltage application.

Acknowledgments

The authors thank Prof. Ken-ichi Nakayama and Dr. Chiho Katagiri in Osaka University for fruitful discussion on photo-CELIV measurement. This work was partially supported by the Advanced Low Carbon Technology Research and Development Program from the Japan Science and Technology Agency, the JSPS KAKENHI Grant Nos. 17K18882 and 15H03552, and JSPS Core-to-Core Program A., Advanced Research Networks.

References

1. Y. Lin, Y. Li, and X. Zhan, "Small molecule semiconductors for high-efficiency organic photovoltaics," *Chem. Soc. Rev.* **41**(11), 4245–4272 (2012).
2. A. Mishra and P. Bäuerle, "Small molecule organic semiconductors on the move: promises for future solar energy technology," *Angew. Chem. Int. Ed.* **51**(9), 2020–2067 (2012).
3. T. Hori et al., "Solution processable organic solar cell based on bulk heterojunction utilizing phthalocyanine derivative," *Appl. Phys. Express* **3**(10), 101602 (2010).
4. M. Ohmori et al., "Crystal structure analysis in solution-processed uniaxially oriented polycrystalline thin film of non-peripheral octahexyl phthalocyanine by grazing incidence wide-angle x-ray scattering techniques," *Appl. Phys. Lett.* **109**(15), 153302 (2016).
5. M. Yoneya et al., "Tilt orientationally disordered hexagonal columnar phase of phthalocyanine discotic liquid crystals," *Phys. Rev. E* **89**(6), 1–8 (2014).
6. M. Ohmori et al., "Molecular packing structure of mesogenic octa-hexyl substituted phthalocyanine thin film by X-ray diffraction analysis," *J. Nanosci. Nanotechnol.* **16**, 3318–3321 (2016).
7. I. Chambrier et al., "X-Ray crystal structure of a mesogenic octa-substituted phthalocyanine," *J. Chem. Soc. Chem. Commun.* 444–445 (1992).
8. M. Ohmori et al., "Single crystal growth and X-ray structure analysis of non-peripheral octahexyl phthalocyanine," *J. Cryst. Growth* **445**, 9–14 (2016).
9. Y. Miyake et al., "High carrier mobility up to 1.4 $cm^2 V^{-1} s^{-1}$ in non-peripheral octahexyl phthalocyanine," *Appl. Phys. Express* **4**(2), 021604 (2011).
10. Q. D. Dao et al., "Effects of processing additives on nanoscale phase separation, crystallization and photovoltaic performance of solar cells based on mesogenic phthalocyanine," *Org. Electron.* **14**(10), 2628–2634 (2013).
11. S. Tiwari and N. C. Greenham, "Charge mobility measurement techniques in organic semiconductors," *Opt. Quantum Electron.* **41**(2), 69–89 (2009).
12. A. Kokil, K. Yang, and J. Kumar, "Techniques for characterization of charge carrier mobility in organic semiconductors," *J. Polym. Sci. Part B Polym. Phys.* **50**(15), 1130–1144 (2012).
13. G. Juška et al., "Extraction current transients: new method of study of charge transport in microcrystalline silicon," *Phys. Rev. Lett.* **84**(21), 4946–4949 (2000).
14. K. Genevičius et al., "Charge transport in π-conjugated polymers from extraction current transients," *Phys. Rev. B* **62**(24), 235–238 (2000).

15. A. J. Mozer et al., "Charge transport and recombination in bulk heterojunction solar cells studied by the photoinduced charge extraction in linearly increasing voltage technique," *Appl. Phys. Lett.* **86**(11), 112104 (2005).
16. A. Pivrikas et al., "A review of charge transport and recombination in polymer/fullerene organic solar cells," *Prog. Photovoltaics Res. Appl.* **15**(8), 677–696 (2007).
17. A. Armin et al., "Injected charge extraction by linearly increasing voltage for bimolecular recombination studies in organic solar cells," *Appl. Phys. Lett.* **101**(8), 083306 (2012).
18. J. C. Swarts et al., "Synthesis and electrochemical characterisation of some long chain 1, 4, 8, 11, 15, 18, 22, 25-octa-alkylated metal-free and zinc phthalocyanines possessing discotic liquid crystalline properties," *J. Mater. Chem.* **11**(2), 434–443 (2001).
19. K. Fukumura et al., "Solvent effects on solution-processable bulk heterojunction organic solar cells utilizing 1, 4, 8, 11, 15, 18, 22, 25-octahexylphthalocyanine," *Jpn. J. Appl. Phys.* **52**, 05DB02 (2013).
20. T. Hori et al., "Non-peripheral octahexylphthalocyanine doping effects in bulk heterojunction polymer solar cells," *Org. Electron.* **13**, 335–340 (2012).
21. T. Shirakawa et al., "Effect of ZnO layer on characteristics of conducting polymer/C60 photovoltaic cell," *J. Phys. D: Appl. Phys.* **37**, 847–850 (2004).
22. S. Morita, A. A. Zakhidov, and K. Yoshino, "Doping effect of buckminsterfullerene in conducting polymer: change of absorption spectrum and quenching of luminescene," *Solid State Commun*. **82**(4), 249–252 (1992).
23. T. Masuda et al., "Acceptor material dependence of photovoltaic properties in bulk heterojunction organic thin film solar cells utilizing soluble octahexylphthalocyanine," *IEEJ Trans. Electron. Inf. Syst.* **132**(11), 1727–1732 (2012) (in Japanese).
24. S. Bange et al., "Charge mobility determination by current extraction under linear increasing voltages: case of nonequilibrium charges and field-dependent mobilities," *Phys. Rev. B* **81**(3), 1–15 (2010).
25. G. Juška et al., "Extraction of photogenerated charge carriers by linearly increasing voltage in the case of Langevin recombination," *Phys. Rev. B* **84**(15), 155202 (2011).
26. T. Usui et al., "Glass-sandwich-type organic solar cells utilizing liquid crystalline phthalocyanine," *Appl. Phys. Express* **10**(2), 021602 (2017).

Yuki Nishikawa graduated in 2017 from the Division of Electronic and Information Engineering, Faculty of Engineering, Osaka University, where he is currently pursuing his master's degree of engineering. He has been engaged in research on charge transport in electrical devices utilizing organic semiconducting materials.

Yuya Nakata received his BE and ME degrees from Osaka University in 2016 and 2018, respectively. Currently, he is working for Glory Ltd.

Shigehiro Ikehara graduated from Kobe City College of Technology in 2013 and received his ME degree from Osaka University in 2015. Currently, he is working for Sony Corporation.

Akihiko Fujii received his PhD in engineering from Osaka University in 1997, After one-year JSPS fellowship, he joined at Department of Electronic Engineering in Osaka University as a research associate in 1998, and was promoted to an associate professor in Division of Electrical, Electronic and Information Engineering in Osaka University in 2006. He has been engaged in research on optical and electrical devices utilizing organic materials including dye molecules and conducting polymers.

Masanori Ozaki received his PhD in engineering from Osaka University in 1988. He joined at Department of Electronic Engineering in Osaka University as a research associate in 1988, and was promoted to an associate professor in 1994 and to a professor in 2005. He has been engaged in the research on physical properties and applications of organic functional materials, particularly liquid crystals, and conjugated polymers.